THE S2C2: FROM SOURCE TO EXTRACTION

J. Van de Walle*[1], M. Abs[1], M. Conjat[2], E. Forton[1], S. Henrotin[1], Y. Jongen[1], W. Kleeven[1],
J. Mandrillon[1,2], P. Mandrillon[1], P. Verbruggen[1]
[1] Ion Beam Applications, Louvain-la-Neuve, Belgium
[2] AIMA, Nice, France

Abstract

The superconducting synchro-cyclotron (S2C2) is the new compact 230 MeV proton cyclotron which will be used in the ProteusONE® proton therapy solution by Ion Beam Applications (IBA). Apart from being the first constructed superconducting cyclotron at IBA, the S2C2 is also the first synchro-cyclotron at IBA. In order to study the beam dynamics in this type of accelerator, new computational tools had to be developed which deal with the much larger number of turns compared to IBA's isochronous cyclotrons, the characteristic longitudinal capture in the central region and the regenerative extraction mechanism. This contribution is structured in four parts. In a first part, the general properties of the S2C2 are discussed (magnetic field, RF frequency, tune, ...). The three following parts discuss in detail the injection, acceleration and extraction.

GENERAL PROPERTIES

The S2C2 is a weak focusing cyclotron with a central field of 5.75 T. The average field as a function of radius is shown in Fig. 1(top). The bottom panel of Fig. 1 shows the first four harmonic components. The first harmonic dominates between the center and 40 cm, whereas all harmonics rise drastically beyond 45 cm due to the presence of the extraction elements, which induce a localized field bump of 1 Tesla. The horizontal and vertical tunes (ν_r and $2\nu_z$) of the S2C2 are shown in Fig. 2 as a function of energy and for different horizontal positions of the superconducting main coil. As can be seen, the Walkinshaw resonance (ν_r=$2\nu_z$) is crossed when the coil is shifted by >2mm away from the regenerator. The precise horizontal main coil positioning is crucial to avoid the Walkinshaw resonance and determines the extracted beam energy (when ν_r=1).

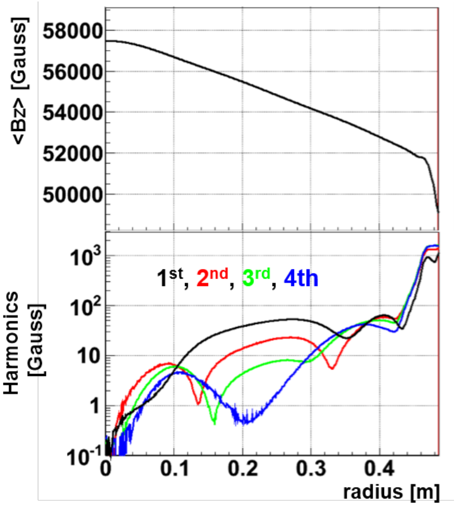

Figure 1: Average magnetic field (top) and first four harmonic components of the magnetic field (bottom) as a function of radius.

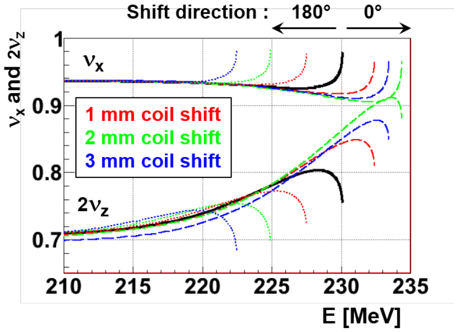

Figure 2: The horizontal tune (ν_r) and twice the vertical tune ($2\nu_z$) as a function of energy for different main coil positions. Black = nominal position, dashed colored = shift away from the regenerator, dotted colored = shift towards the regenrator.

The RF frequency varies from around 90 to 60 MHz, covering the injection and extraction frequencies at 87.6 and 63.2 MHz, resp. One full RF frequency cycle (1 ms) is shown Fig. 3.

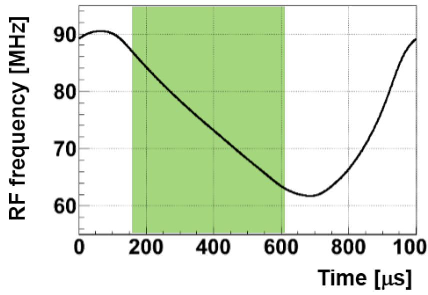

Figure 3: One period (1 ms) in the RF frequency cycle. The acceleration period is indicated in green and lasts about 450 µs.

Figure 4 shows a magnetic field map in the median plane and the position of the regenerator, the septum, the extraction channel and the yoke penetrations for the three horizontal tie rods.

---

[*] jarno.vandewalle@iba-group.com

ISBN 978-3-95450-167-0

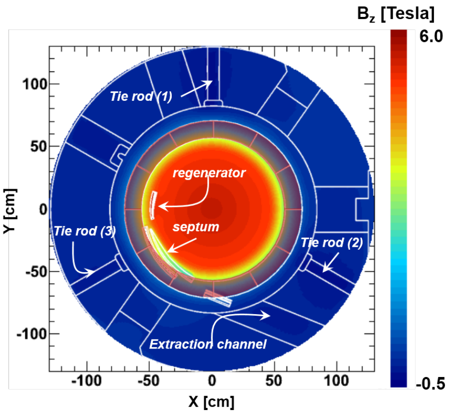

Figure 4: Complete magnetic field map (measured + simulated). Positions of the regenerator, the tie rod yoke penetrations, the septum and the extraction channels are shown.

INJECTION

Due to the small injection energy and the high central magnetic field, the first turn in the S2C2 has a radius of only 3 mm. Figure 5 shows the off-centering of protons after 30 turns in the S2C2 as a function of their initial RF phase at injection. The RF phase convention is shown in the inset. During injection, the phase acceptance ranges from 20 to 90 degrees. During acceleration, the stable phase range is 20 to 260 degrees, as determined by the separatrix. When the source is perfectly centered, the orbit centering is not dependent on the initial RF phase, nor on the applied dee voltage. When the source is shifted by 1 mm, the orbit centering depends strongly on the initial RF phase and on the applied dee voltage (see Fig. 5 - open symbols). The bottom panels of Fig. 5 shows the beam profile at the end of the "energy selection system" in the gantry of the ProteusONE$^{\circledR}$ system. At this position, the dispersion is maximized and we have a good image of the energy distribution in the beam ($\approx$130 keV/mm). The open and filled symbols refer to an off-centered and centered source, resp. The mean energy shifts by about 160 keV and the energy spread is higher for an off-centered source. The top panel of Fig. 6 shows the distribution of the protons in the stable separatrix at 3 MeV, or, equivalently 8 µs after the reference time, defined as the time when the RF frequency equals the cyclotron frequency in the center of the S2C2. The lower panel shows the relative time (with respect to the reference time) at which the proton was captured at the source. The total capture time is $\approx$6 µs and protons which are captured "late", reside near the borders of the separatrix and risk to fall out of the stable separatrix, if the total "bucket area" reduces during acceleration.

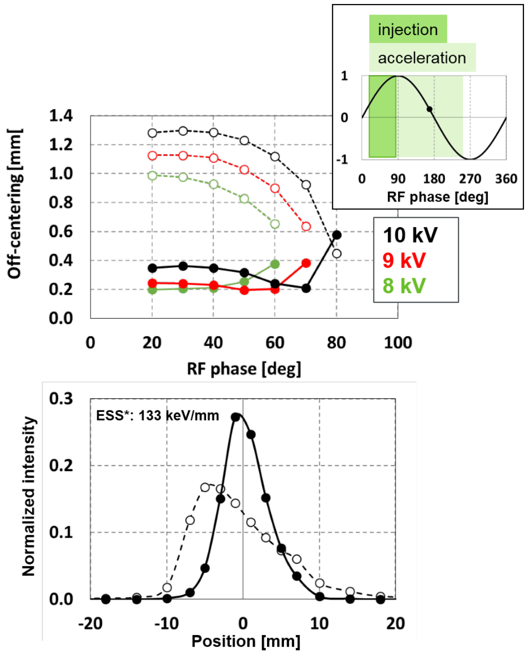

Figure 5: (Top) Orbit off-centering as a function of dee voltage and source position : (filled symbols) centered source (open symbols) 1 mm shifted source. The inset shows the accepted RF phase range at injection and during acceleration. (Bottom) energy distribution at the end of the Energy Selection System (*ESS) in the gantry.

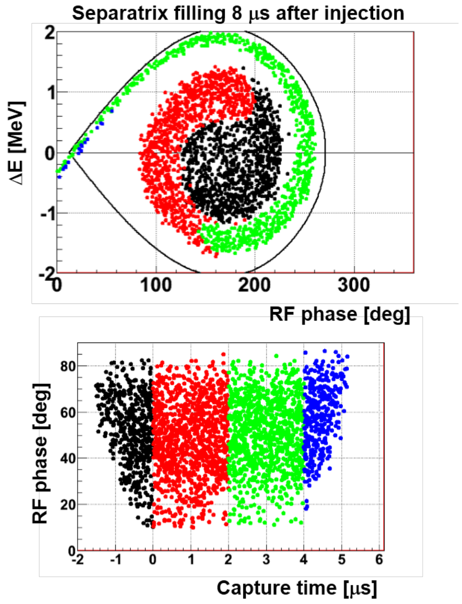

Figure 6: (Top) Filling of the longitudinal separatrix at 3 MeV. (Bottom) the accepted RF phases at injection as a function of the relative injection time. The color codes indicate the link between capture time and position inside the separatrix.

ACCELERATION

A synchronous proton will make $\approx$40000 turns in the S2C2 from the source up to extraction. With the "Advanced Orbit Code" (see [1] and [2]), the equations of motion are integrated precisely as a function of time. The precision of the integration process comes at the cost of high computation time. Simulating a statistically relevant amount of protons in order to deduce beam properties or to study the impact of perturbations in the S2C2 (radial fields, magnetic harmonics, source shifts, etc ...) would require too much time. Therefore, a new code was developed which tracks only the relevant parameters during acceleration: the RF phase, the energy and the orbit center coordinates. This code is referred to as the "phase motion code". The equations of motion for the energy and RF phase are :

$$\frac{dE}{dt} = eF_{RF}V_{RF}\,sin(\phi) \quad (1)$$

$$\frac{d\phi}{dt} = 2\pi(F_{RF} - F_p) \quad (2)$$

where E and e are the kinetic energy and charge of the proton, F_{RF} is the RF frequency, F_p the revolution frequency of the proton, V_{RF} the RF voltage and ϕ the RF phase of the proton. One proton was simulated in AOC from the source up to extraction (calculation time ≈30 min). The properties of the proton, 10 µs after initial capture were input as initial conditions to the "phase motion" code. The energy as a function of time, calculated with "AOC" and "phase motion" is shown in Fig. 7 in black and red (resp.) and the similarity is good. The equations of motion for the orbit center coordinates (x_c and y_c) in "phase motion" are derived from the following Hamiltonian (see [3])

$$\begin{aligned}
H(x_c, y_c) &= \frac{1}{2}(\nu_r - 1)(x_c^2 + y_c^2)\\
&+ \frac{r}{2}(A_1 x_c + B_1 y_c) + [D_3 x_c + D_4 y_c][x_c^2 + y_c^2]\\
&+ \frac{1}{4}(A_2 + \frac{1}{2}A_2')(x_c^2 - y_c^2) + \frac{1}{2}(B_2 + \frac{1}{2}B_2')x_c y_c\\
&+ \frac{1}{48r}(D_1[4x_c^3 - 3x_c(x_c^2 + y_c^2)] + D_2[3y_c(x_c^2 + y_c^2) - 4y_c^3])\\
&+ O(4)
\end{aligned}$$

where the first line includes parameters related to the average field, the second, third and fourth line include parameters related to the first, second and third harmonics (and their derivatives, see [3]). The result of the integration of the equations of motion derived from the above Hamiltonian is shown in Fig. 8. The figure compares the orbit center coordinates of all stable closed orbits (green line), the orbit center evolution of an accelerated proton calculated in AOC (black line) and the orbit center coordinates integrated in the "phase motion" code (red line). In the top figure, the average field and the first harmonic are taken into account, in the bottom figure also the second and third harmonics are taken into account in the "phase motion" code. This illustrates that the evolution of the orbit centers in the S2C2 is fully determined by the first harmonic and the average field up to around 225 MeV. Beyond this energy, more harmonics need to be taken into account to accurately describe the evolution of the orbit center, illustrating the effect of the regenerator (see also Fig. 1) and the instability of the orbit center when approaching the $2\nu_r$=2 resonance.

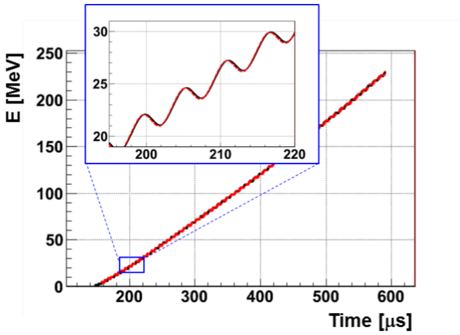

Figure 7: Calculated evolution of the proton energy versus time : (black) "AOC" (red) "phase motion". See text for details.

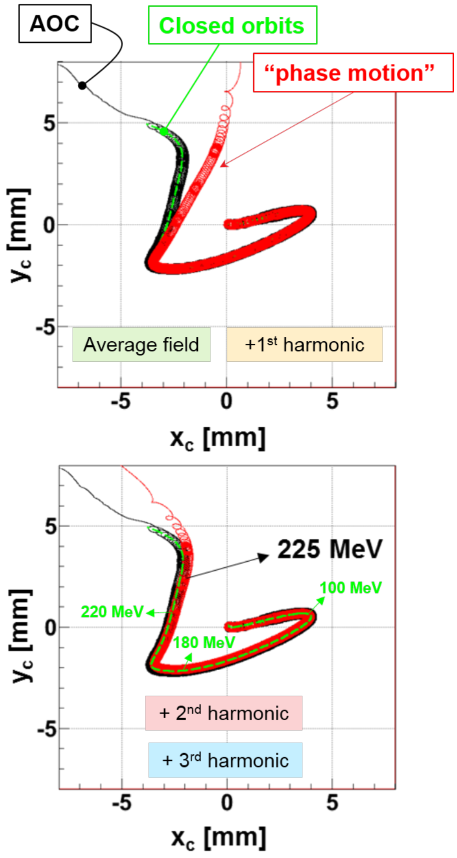

Figure 8: (Green) closed orbit centers for all energies. (Black) evolution of the orbit center for a proton simulated in AOC from source to extraction. (Red) evolution of the orbit center, calculated in "phase motion", with initital conditions at 3 MeV taken from AOC : (top) average field and first harmonic (bottom) second and third harmonic also included.

The phase motion code allows to study what happens to a proton which falls out of the stable separatrix, since the beam properties can be tracked over several RF frequency sweeps (ms range). Figure 9 shows how the energy of such a lost proton fluctuates over two RF frequency sweeps. Clearly, when the RF frequency equals the revolution frequency of the proton, the energy changes resonantly, but the proton is not recaptured

ISBN 978-3-95450-167-0

in the stable separatrix. The bottom part of Fig. 9 shows a statistical distribution of the energy gained or lost by a proton when the RF frequency equals its revolution frequency. The blue and red curves correspond to energy changes on the falling and rising edge of the frequency curve, resp. On average, energy is lost on the falling edge and energy is gained on the rising edge. Since the dee voltage is set to a lower value when the frequency is rising, the effect of energy gain is minimized and on average there is no energy gain.

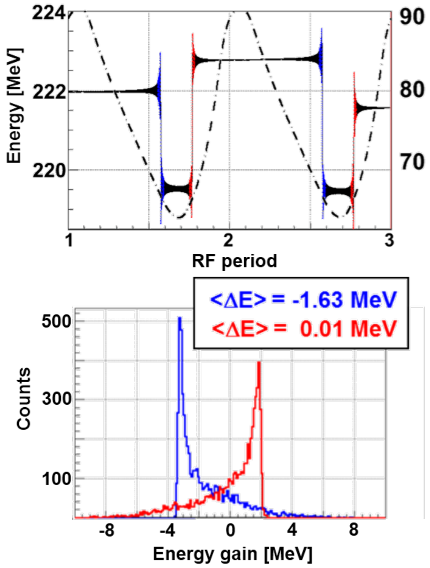

Figure 9: (Top) evolution of the energy of a lost proton during 2 RF frequency cycles. (Bottom) statistical energy change of the proton over 20 RF frequency cycles on the falling and rising frequency flank (blue and red, resp.).

EXTRACTION

Before the beam can be extracted from the S2C2, the main coil has to be aligned vertically in order to eliminate radial fields in the median plane. From AOC simulations, we deduced a position inside the S2C2 where the radial orbit displacement near extraction is maximized and the effect of a vertically misaligned coil is seen in the last turn of the proton. Figure 10 shows a comparison of two irradiated gafchromic films inside the S2C2 where the coil was 0.5 mm too low (middle) and well aligned (top). The bottom figure shows the simulated (AOC) effect of a 0.5 mm vertically misaligned coil on the vertical displacement of the last turn. The observation of the linearity between vertical displacement of the last turn at this position in the S2C2 and the vertical coil displacement facilitates the vertical alignment of the coil.

From Fig. 9 it is clear that "lost protons" can gain enough energy to be extracted on the rising edge of the frequency curve, on the condition that they are lost close to the extraction energy. The latter condition was achieved experimentally by dropping the dee voltage very close to extraction. Figure 11(top) shows a "standard" dee voltage profile where the dee voltage is lowered at the minimum RF frequency

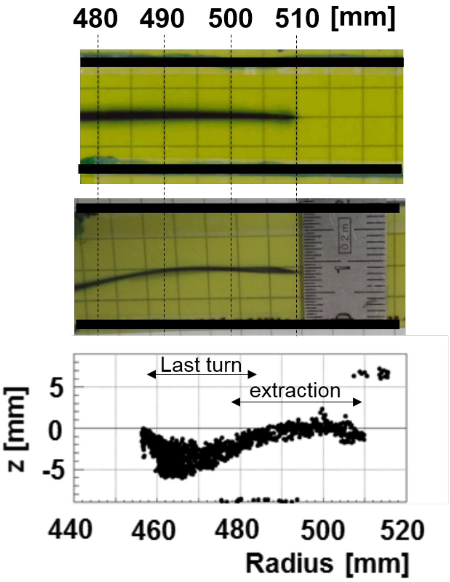

Figure 10: Measured (top) and simulated (bottom) vertical displacement of the beam in the last turn due to a 0.5 mm vertical misalignment of the main coil.

(green) and one profile, where the dee voltage is lowered very close to the extraction frequency (red). The signal observed on a "poly crystalline diamond probe" (pCVD, see [4] and [5]) is shown in the lower 2 panels of Fig. 11. With a "standard" dee voltage profile, beam is observed only at the extraction frequency on the falling edge (middle panel of Fig. 11). When the dee voltage is dropped close to extraction, two small peaks are observed around the "normal" extraction frequency. Consistent with the results of the phase motion code, protons are extracted at the extraction frequency on the rising edge of the frequency curve. The second peak before the extraction frequency are "lost protons" which get extracted because of a resonance in their orbit center coordinates (=emittance blow up in the S2C2). This can be understood from the equations of motion of the orbit center coordinates, which have the form

$$\frac{dx_c}{dt} = (\nu_r - 1)y_c + \alpha x_c + \beta y_c + \ldots$$
$$\frac{dy_c}{dt} = (\nu_r - 1)x_c + \alpha' x_c + \beta' y_c + \ldots$$

where the coefficients α,β,α' and β' contain harmonic components of the magnetic field, which are related to the energy via the radius on which the harmonics are evaluated and the magnetic rigidity of a proton at that radius. In first order, the orbit center oscillates with a frequency equal to (ν_r-1)F$_p$ and the energy (and thus the coefficients α,β,α' and β') oscillates with a frequency equal to F$_{RF}$-F$_p$. A resonance can occur when

$$F_{RF} = F_p \pm (\nu_r - 1)F_p$$

In AOC and phase motion, such a resonance of the orbit center was indeed observed. The AOC calculation is shown

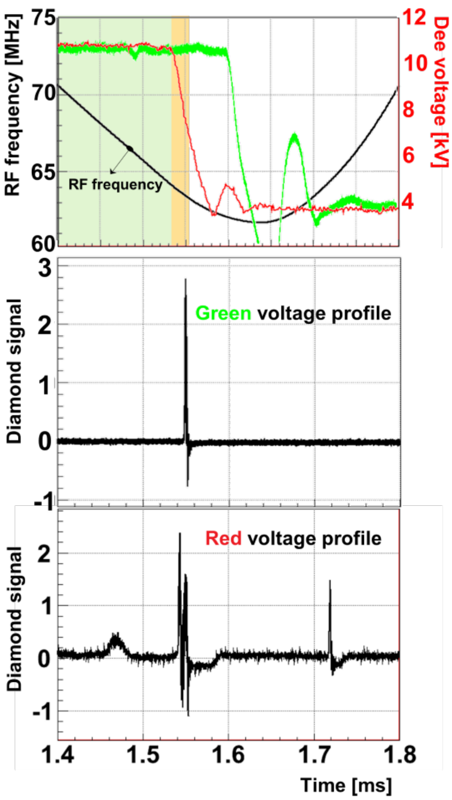

Figure 11: (Top) The frequency curve and two dee voltage profiles. (Middle) Extracted beam for the "standard" dee voltage profile. (Bottom) Extracted beam for the "red" voltage profile. See text for details.

in Fig. 12, where the proton is extracted due to instability of its orbit center exactly at the RF frequency corresponding to F_{RF}=F_p+(ν_r-1)F_p.

With the knowledge of what happens to "lost protons", an effort was made to avoid at all cost that protons are lost near extraction. This is accomplished by keeping the total bucket area increasing or constant during the acceleration.The bucket area is calculated with the following input parameters: the measured dee voltage, the measured derivative of the RF frequency and a variety of derived quantities from a closed orbit analysis (relation between F_p, energy, time, etc ...). Combining results from AOC calculations in the central region, "phase motion" calculations from 3 MeV to 225 MeV and AOC calculations from 225 MeV to extraction, all extracted beam properties can be calculated. Table 1 compares measured and calculated extracted beam properties.

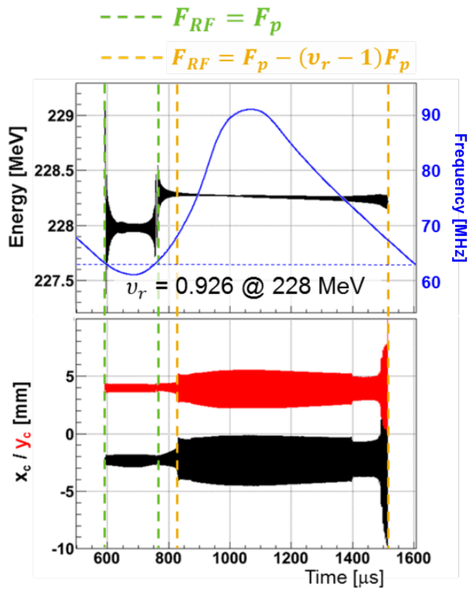

Figure 12: AOC simulation of a lost proton close to extraction : (top) energy resonances when the RF frequency equals the revolution frequency of the proton and (bottom) resonances in the orbit center coordinates, leading to extraction due to orbit center instability.

Table 1: Measured and Simulated Extracted Beam Properties

Property	**simulated**	**measured**
Energy spread	150 keV	≈400 keV
$\Delta E/\Delta I_{coil}$	440 keV/A	440 keV/A
ΔE/(mm source shift)	200 keV/mm	≈200 keV/mm
Pulse duration	8 µs	8 µs
Extraction efficiency	50 %	≈35 %
Horizontal emittance	20 π mm mrad	23.2 π mm mrad
Vertical emittance	4 π mm mrad	3.2 π mm mrad

CONCLUSION

In order to study the extracted beam properties of the S2C2 we have developed different computational tools. These new tools have enabled us to study the orbit centering and its impact on the extraction process and have given new insights in the evolution of protons which fell out of the stable bucket area during acceleration. The acquired in-depth understanding of beam dynamics inside the S2C2 is important to make it a reliable and controlled medical accelerator.

REFERENCES

[1] W. Kleeven *et al.*, "AOC, A Beam Dynamics Design Code for Medical and Industrial Accelerators at IBA", in *Proc. IPAC'16*, paper TUPOY002.

[2] W. Kleeven *et al.*, "Overview of Recent Progress of Simulations for Cyclotrons", presented at Cyclotrons'16, Zurich, Switzerland, Sep. 2016, paper WEA01, this conference.

[3] H.L. Hagedoorn and N.F. Verster, NIM **18,19** (1962) p.201-228

[4] J. Van de Walle *et al.*, "A Diamond Detector Test Bench to Assess the S2C2 Beam Characteristics", presented at Cyclotrons'16, Zurich, Switzerland, Sep. 2016, paper MOP19, this conference.

[5] Cividec, `https://cividec.at`